Energy-Storage Devices

International Edition: DOI: 10.1002/anie.201501261
German Edition: DOI: 10.1002/ange.201501261

# Aqueous Manganese Dioxide Ink for Paper-Based Capacitive Energy Storage Devices**

*Jiasheng Qian, Huanyu Jin, Bolei Chen, Mei Lin, Wei Lu, Wing Man Tang, Wei Xiong, Lai Wa Helen Chan, Shu Ping Lau, and Jikang Yuan**

***Abstract:*** *We report a simple approach based on a chemical reduction method to synthesize aqueous inorganic ink comprised of hexagonal $MnO_2$ nanosheets. The $MnO_2$ ink exhibits long-term stability and continuous thin films can be formed on various substrates without using any binder. To obtain a flexible electrode for capacitive energy storage, the $MnO_2$ ink was printed onto commercially available A4 paper pretreated with multiwalled carbon nanotubes. The electrode exhibited a maximum specific capacitance of 1035 $F g^{-1}$ (91.7 $mF cm^{-2}$). Paper-based symmetric and asymmetric capacitors were assembled, which gave a maximum specific energy density of 25.3 $Wh kg^{-1}$ and a power density of 81 $kW kg^{-1}$. The device could maintain a 98.9 % capacitance retention over 10000 cycles at 4 $A g^{-1}$. The $MnO_2$ ink could be a versatile candidate for large-scale production of flexible and printable electronic devices for energy storage and conversion.*

Printable electronics is of great interest in areas ranging from thin-film transistors (TFTs), energy-storage devices, solar cells, to micro-electromechanical systems (MEMS).[1] For example, the preparation of various inks composed of semiconductors, biological materials, carbon, and conductive oxides have been reported.[2] In particular, as a consequence of its abundance, high theoretical capacity, and environmental compatibility, manganese dioxide ($MnO_2$) is usually regarded as an ideal candidate for the electrode materials of portable devices, water treatment, up-conversion, as well as photocatalysis.[3] Conventional $MnO_2$ electrodes are mainly prepared by two approaches: 1) nanostructured $MnO_2$ or $MnO_2$-containing composite precipitates are generated by wet chemical processes[3a,b,4] or 2) by direct electrodeposition or chemical deposition on various substrates (e.g. glass, quartz, copper, or aluminum foil).[5] These existing preparation methods suffer from high cost, complicated processes, and superfluous contaminations. On the other hand, the introduction of insulating binders during the coating process can cause agglomeration in the inks, thereby leading to a reduction of the electrical conductivity.[2a] It still remains a great challenge to synthesize $MnO_2$ inks with high reliability and versatility. Hence, the development of environmentally benign aqueous $MnO_2$ inks is desirable for highly efficient and large-scale printable processes. Nevertheless, few studies on aqueous $MnO_2$ inks have been reported to date.[6]

Herein, we report a simple route to synthesize aqueous $MnO_2$ ink comprised of hexagonal $MnO_2$ nanosheets (*h*-MnNSs). The aqueous $MnO_2$ ink was synthesized by a simple liquid-phase process at room temperature. First, highly crystalline carbon particles with diameters of about 200 nm (see Figure S1 in the Supporting Information) were prepared as the template by the microwave hydrothermal method. Then, the as-prepared carbon particles were oxidized by $KMnO_4$ to form the $MnO_2$ nanosheets through a morphology transmission mechanism.[7] The as-prepared $MnO_2$ ink (1 $mg mL^{-1}$) had a dark brown color (Figure 1 A). The concentration of $MnO_2$ ink can be increased up to about 1.5 $mg mL^{-1}$, which is suitable for large mass loading. The $MnO_2$ ink can be coated onto commercial printing paper with

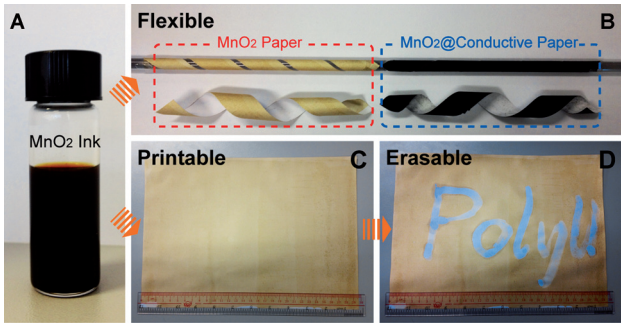


***Figure 1.*** Performance tests of inorganic $MnO_2$ ink. A) Photograph of the $MnO_2$ ink. B) Flexible paper strips coated with $MnO_2$ ink with (right) and without (left) treatment with MWCNTs. C) A sheet of A4-sized paper coated by the $MnO_2$ ink. D) The $MnO_2$ coated paper shown in (C) erased by oxalic acid, with the erased area showing the word "PolyU".

[*] J. Qian,[+] H. Jin,[+] Dr. B. Chen, M. Lin, Dr. W. Lu, Dr. W. M. Tang, Prof. L. W. H. Chan, Prof. S. P. Lau, Dr. J. Yuan
Department of Applied Physics
The Hong Kong Polytechnic University
Hong Kong SAR
E-mail: jikang.yuan@polyu.edu.hk
Dr. W. Xiong
School of Chemistry and Environmental Engineering
Wuhan Institute of Technology
693 Xiongchu Road, Wuhan 430073 (P.R. China)
Prof. S. P. Lau
Shenzhen Research Institute
The Hong Kong Polytechnic University
Shenzhen 518057 (P.R. China)
[+] These authors contributed equally to this work.

[**] This work was financially supported in part by the Research Grants Council (RGC) of Hong Kong through the General Research Fund (project nos. PolyU 5292/12E and PolyU 153012/14P), the Hong Kong Polytechnic University (grant nos. 1-ZV5K, 1-ZE14, and 1-ZV9B), and National Natural Science Foundation of China (NSFC, grant no. 11374250). We thank Chi Man Luk and Dr. Yi Ching Cheung for their assistance during the measurements.

Supporting information for this article is available on the WWW under http://dx.doi.org/10.1002/anie.201501261.

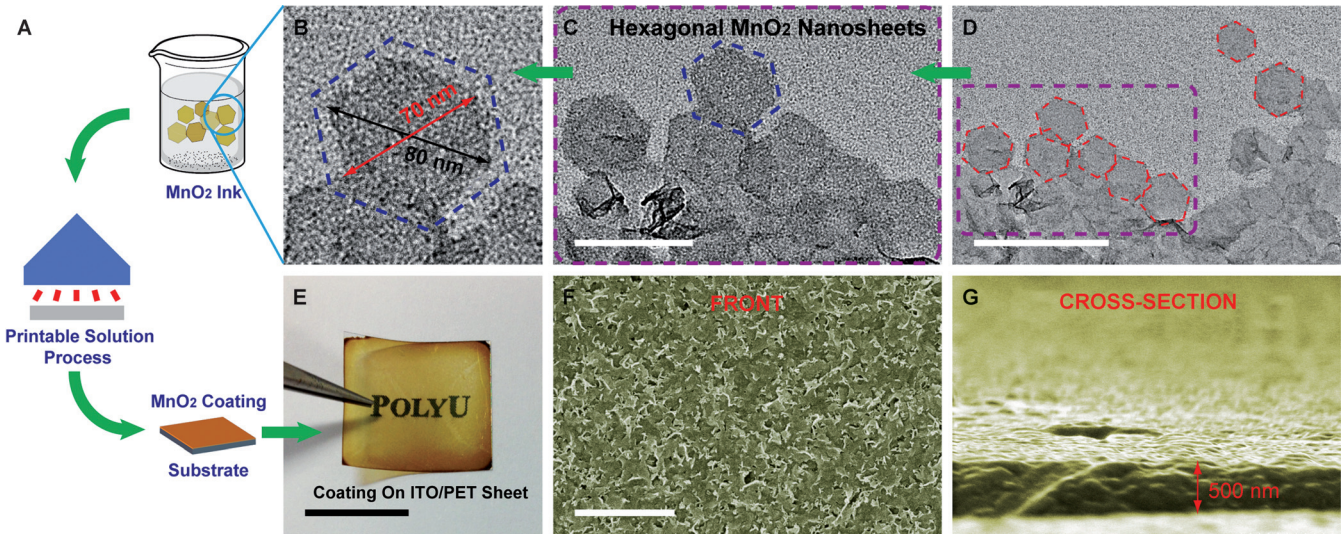


***Figure 2.*** Illustration of the solution-processable $MnO_2$ ink. A) Schematic diagram of the printing process. B) HRTEM image of a single *h*-MnNS. C) TEM image showing the *h*-MnNSs. Scale bar: 100 nm. D) TEM image of the large-scale *h*-MnNSs. Scale bar: 200 nm. E) Photograph of an ITO/PET sheet with a $MnO_2$ coating. Scale bar: 1 cm. F,G) SEM images of the front and cross-sectional parts of the $MnO_2$/ITO/PET sheet in (E). Scale bar: 1 μm.

and without treatment with multiwalled carbon nanotubes (MWCNTs; Figure 1 B,C). In contrast to other inks, the $MnO_2$ ink could be selectively etched out by a 1 M oxalic acid solution without damaging the substrate (Figure 1 D). Such an erasable property cannot be realized with the previously reported inks.[6] The erasable $MnO_2$ ink could be a potential candidate for transient coating or electrode materials when applied in "epidermal electronics" or "transient electronics".[8]

Low- and high-resolution transmission electron microscopy (TEM) images (Figure 2 B–D and see Figure S2 in the Supporting Information) reveal the hexagonal $MnO_2$ nanosheets (*h*-MnNSs) with diameters ranging from 60 to 90 nm. Furthermore, clear edges of the nanosheets can be observed (Figure 2 B). The thickness of the *h*-MnNSs was estimated to be about 3.6 nm by electron energy loss spectroscopy (EELS, see Figure S3 in the Supporting Information). The X-ray diffraction (XRD) pattern of the sample indicates a layered birnessite-type structure (see Figure S4 in the Supporting Information). The Raman spectrum of $MnO_2$ shows two peaks located at 564 and 633 $cm^{-1}$ (see Figure S5 in the Supporting Information), and the peaks can be assigned to Mn-O lattice vibrations.[9]

The zeta potential spectrum shows the $MnO_2$ nanosheets are negatively charged in water (see Figure S9 in the Supporting Information) and they can be homogeneously dispersed in water as a result of the electrostatic interaction between the *h*-MnNSs and $K^+$ ions. The $MnO_2$ ink tends to form continuous thin films on smooth substrates (Figure 2 A,E). Figure 2 E shows a photograph of a piece of a $MnO_2$-coated indium tin oxide coated polyethylene terephthalate (ITO/PET) sheet with a mass loading of 0.25 mg $cm^{-2}$. The $MnO_2$/ITO/PET sheet was placed on a paper marked with "POLYU". The UV/Vis spectrum shows that the sheet exhibits high transparency (see Figures S11 and S12 in the Supporting Information). Figure 2 F,G show the scanning electron microscopy (SEM) images of the front and cross-sectional parts of the $MnO_2$ coating, respectively. The compacted thin films exhibit an average thickness of approximately 500 nm.

The $MnO_2$ ink was first studied as the electrode material. Conductive paper with a sheet resistance of about 30 Ω $sq^{-1}$ was used as the current collector and substrate for printing with $MnO_2$ ink. The conductive paper was prepared by coating MWCNTs onto the commercial paper. Figure 3 B shows the $MnO_2$ ink coated on a piece of conductive paper with dimensions of $1 \times 1$ $cm^2$. The corresponding SEM images of the cross-sectional and front parts of the paper coated with $MnO_2$ nanosheets (Figure 3 A,C, respectively) show a large quantity of $MnO_2$ nanosheets with a thickness of about 70 μm to be deposited on the MWCNT layer. A series of $MnO_2$ paper (MnPaper) electrodes with a mass loading of 40, 80, and 176 μg $cm^{-2}$ (denoted as MnPaper-40, MnPaper-80, and MnPaper-176, respectively) were prepared for measurement of the electrochemical performances by using a three-electrode system in 0.5 M $Na_2SO_4$ solution. A platinum electrode and an Ag/AgCl electrode were used as the counter electrode and the reference electrode, respectively. The cyclic voltammetry (CV) curves of the different MnPaper electrodes at 10 mV $s^{-1}$ (Figure 3 D) show rectangular-like curve shapes. Such shapes are attributed to high-speed ion transport on the electrode/electrolyte interface with rapid charging and discharging characteristics. The process is based on a redox reaction according to Equation (1).[10]

$$MnO_2 + x\,H^+ + y\,Na^+ + (x+y)e^- \leftrightarrow MnOOH_xNa_y \qquad (1)$$

Notably, the calculated specific capacitance of the MnPaper-80 electrode reached the highest value of 642.5 F $g^{-1}$ at 10 mV $s^{-1}$. This value is about two orders of magnitude higher than that of the pure MWCNTs electrode (6.94 F $g^{-1}$). Such an

  

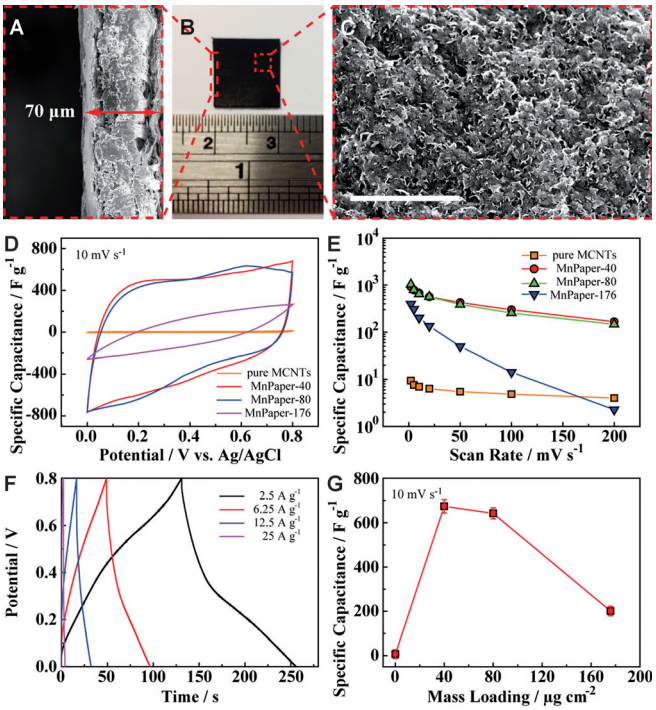


***Figure 3.*** Electrochemical performances of the $MnO_2$@conductive paper electrode. A) SEM image of the cross-sectional part of the $MnO_2$@conductive paper. B) Optical photograph of the $1\times1$ $cm^2$ MnPaper electrode. C) SEM image of the conformal $MnO_2$ coating on the conductive paper. Scale bar: 1 μm. D) CV curves of the MnPaper electrodes with different mass loadings at 10 $mV\,s^{-1}$. E) Specific capacitance ($C_{sp}$) versus scan rate for the pure MWCNTs electrode and for MnPaper electrodes with different mass loadings. F) GCD curves of the MnPaper-80 electrode at different current densities of 2.5, 6.25, 12.5, and 25 $A\,g^{-1}$. G) Specific capacitance versus mass loading of different MnPaper electrodes. The specific capacitances are estimated from the CV curves at 10 $mV\,s^{-1}$.

enhanced performance is attributed to the conformal coating of $MnO_2$ ink contributing huge pseudocapacitance. The specific capacitances of the MnPaper electrodes were calculated based on the profiles of the CV curves versus different scan rates (Figure 3E). A maximum specific capacitance of 1035 $F\,g^{-1}$ (91.7 $mF\,cm^{-2}$) was achieved by the MnPaper-80 electrode at 2 $mV\,s^{-1}$. This value is about 100 times higher than that of the pure MWCNTs electrode (9.4 $F\,g^{-1}$, 8.9 $mF\,cm^{-2}$) and is almost equal to or higher than those of the reported $MnO_2$ electrodes.[11] This value almost approaches the theoretical value of 1370 $F\,g^{-1}$ for the $MnO_2$ electrode.[11a] When the scan rate reached 100 $mV\,s^{-1}$, the specific capacitance of the MnPaper-80 electrode still retained a reasonable value of 255 $F\,g^{-1}$. In contrast, the specific capacitance of the MnPaper-176 electrode decreased dramatically to a value even lower than that of the pure MWCNTs electrode at 200 $mV\,s^{-1}$ because of excess $MnO_2$ causing poor electrical conductivity. The galvanostatic charge/discharge (GCD) characteristics of the MnPaper-80 electrode were consistent with those of the CV measurements (Figure 3F). A pair of redox peaks appeared in the GCD curves as a result of the formation of $Na_xMnO_2$ on the electrode, as expected.[10b] This result agrees with that from the CV curves in Figure 3D, and is further consistent with the XRD pattern (see Figure S4 in the Supporting Information). Furthermore, when a high current density of 25 $A\,g^{-1}$ was applied, the MnPaper-80 electrode could still reach a capacitance value as high as 572.5 $F\,g^{-1}$ (48.8 $mF\,cm^{-2}$), thus indicating that the electrode can be a potential candidate for application in high-power devices.[12] The profiles of the specific capacitance of different MnPaper electrodes at 10 $mV\,s^{-1}$ versus mass loading of $MnO_2$ are shown in Figure 3G. As the mass loading of $MnO_2$ increased, the specific capacitance of the MnPaper-40 electrode increased significantly compared to that of the pure MWCNTs electrode. There was no apparent drop in the high specific capacitance when the mass loading was increased to 80 $\mu g\,cm^{-2}$. This phenomenon further demonstrates that the $MnO_2$ and the MWCNTs were mixed homogeneously on the paper. When the mass loading of $MnO_2$ reached 176 $\mu g\,cm^{-2}$, the specific capacitance of the MnPaper electrode fell sharply, but could still maintain a value of about 200 $F\,g^{-1}$.

The capability of the $MnO_2$ ink was further demonstrated by assembling a paper-based symmetric capacitor (SC). The two MnPaper-80 electrodes were sandwiched by a polyvinyl alcohol (PVA)/LiCl quasisolid-state electrolyte and a separator (Figure 4A). The CV curves of the MnPaper-80 SC at different scan rates (Figure 4B) exhibit ideal rectangular shapes and high-rate reversibility at 100 $mV\,s^{-1}$. A specific capacitance of 147 $F\,g^{-1}$ (588 $F\,g^{-1}$ for a single electrode) was measured at 10 $mV\,s^{-1}$. This value is close to the capacitance value measured in the three-electrode system. Furthermore, a 90° bending test and a serial–parallel connection test were performed (see Figure S15 in the Supporting Information). The MnPaper-80 SC was also shown to undergo 10000 charge/discharge cycles at 4 $A\,g^{-1}$ with a retention of 98.9% capacitance (Figure 4C), thus indicating a prolonged lifetime.

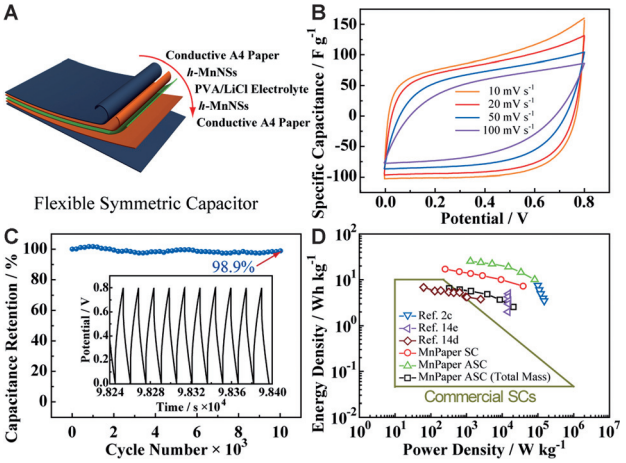


***Figure 4.*** Electrochemical performances of the MnPaper-80 SC. A) Schematic illustration of the structure of the SC cell. B) CV curves of the SC at 10, 20, 50, and 100 $mV\,s^{-1}$. C) Capacitance retention of the SC over 10000 cycles. Inset: Charge/discharge curves for the last ten cycles. D) Energy and power densities (Ragone plots) of the SC operated at 0.8 V and the ASC operated at 1.8 V (active material only and total mass including all dead components) compared with SWCNTs conductive paper SC: 0.8 V (Ref. [2a]), graphene/$MnO_2$ SC: 1 V (Ref. [13d]), and $MnO_2$/carbon nanoparticles SC: 0.8 V (Ref. [13e]).

Figure 4D shows the Ragone plots for a comprehensive comparison of the energy and power density between the MnPaper-80 capacitors and some recently reported typical capacitors (see Table S1 in the Supporting Information). The specific energy density of 17 $Wh\,kg^{-1}$ and the power density of 38 $kW\,kg^{-1}$ for the MnPaper-80 SC are higher than values reported in the literature.[13] To further optimize the energy and power densities of the paper-based capacitor, a MnPaper-80 asymmetric capacitor (MnPaper-80 ASC) was assembled (see Figure S18 in the Supporting Information). The values of the energy and power density of the ASC could reach up to 25.3 $Wh\,kg^{-1}$ and 81 $kW\,kg^{-1}$, respectively. The performance of the ASC can be attributed to the coaxial structure and the homogeneous $MnO_2$ coating on the conductive paper.

In summary, aqueous $MnO_2$ ink was prepared by a facile synthetic route. The $MnO_2$ ink exhibits long-term stability and printability on a wide range of different substrates. The electrochemical performances of $MnO_2$-coated paper electrodes were also examined. Furthermore, both paper-based symmetric and asymmetric capacitors were assembled. The specific capacitance, specific energy and power densities of the paper-based capacitor could reach 1035 $F\,g^{-1}$ (91.7 $mF\,cm^{-2}$), 25.3 $Wh\,kg^{-1}$, and 81 $kW\,kg^{-1}$, respectively. The device could achieve a capacitance retention of up to 98.9% over 10000 cycles at 4 $A\,g^{-1}$. All these advantages of the $MnO_2$ ink make it a versatile candidate for the large-scale production of high-performance electronic devices in the near future.

**Keywords:** electrochemistry · energy-storage devices · metal oxides · $MnO_2$ ink · thin films

**How to cite:** *Angew. Chem. Int. Ed.* **2015**, *54*, 6800–6803
*Angew. Chem.* **2015**, *127*, 6904–6907

[1] a) S. T. Meyers, J. T. Anderson, C. M. Hung, J. Thompson, J. F. Wager, D. A. Keszler, *J. Am. Chem. Soc.* **2008**, *130*, 17603–17609; b) D. Tobjörk, R. Österbacka, *Adv. Mater.* **2011**, *23*, 1935–1961; c) K. K. Banger, Y. Yamashita, K. Mori, R. L. Peterson, T. Leedham, J. Rickard, H. Sirringhaus, *Nat. Mater.* **2011**, *10*, 45–50; d) J. van Embden, A. S. R. Chesman, E. D. Gaspera, N. W. Duffy, S. E. Wathins, J. J. Jasieniak, *J. Am. Chem. Soc.* **2014**, *136*, 5237–5240.

[2] a) L. Hu, J. W. Choi, Y. Yang, S. Jeong, F. L. Mantia, L.-F. Cui, Y. Cui, *Proc. Natl. Acad. Sci. USA* **2009**, *106*, 21490–21494; b) J. Wang, K. K. Manga, Q. Bao, K. P. Loh, *J. Am. Chem. Soc.* **2011**, *133*, 8888–8891; c) J. Liang, M. Castronovo, G. Scoles, *J. Am. Chem. Soc.* **2012**, *134*, 39–42; d) Y. Xu, M. G. Schwab, A. J. Strudwick, I. Hennig, X. Feng, Z. Wu, K. Müllen, *Adv. Energy Mater.* **2013**, *3*, 1035–1040; e) J. Song, J. Li, J. Xu, H. Zeng, *Nano Lett.* **2014**, *14*, 6298–6305; f) Z. Liu, K. Parvez, R. Li, R. Dong, X. Feng, K. Müllen, *Adv. Mater.* **2015**, *27*, 669–675; g) J. Song, S. A. Kulinich, J. Li, Y. Liu, H. Zeng, *Angew. Chem. Int. Ed.* **2015**, *54*, 462–466; *Angew. Chem.* **2015**, *127*, 472–476.

[3] a) Q. Qu, P. Zhang, B. Wang, Y. Chen, S. Tian, Y. Wu, R. Holze, *J. Phys. Chem. C* **2009**, *113*, 14020–14027; b) A. Sumboja, C. Y. Foo, X. Wang, P. S. Lee, *Adv. Mater.* **2013**, *25*, 2809–2815; c) M. Xue, L. Huang, J.-Q. Wang, Y. Wang, L. Gao, J.-H. Zhu, Z.-G. Zou, *Nanotechnology* **2008**, *19*, 185604–185612; d) R. Deng, X. Xie, M. Vendrell, Y.-T. Chang, X. Liu, *J. Am. Chem. Soc.* **2011**, *133*, 20168–20171.

[4] a) Z.-S. Wu, W. Ren, D.-W. Wang, F. Li, B. Liu, H.-M. Cheng, *ACS Nano* **2010**, *4*, 5835–5842; b) Z. Fan, J. Yan, T. Wei, L. Zhi, G. Ning, T. Li, F. Wei, *Adv. Funct. Mater.* **2011**, *21*, 2366–2375; c) M.-K. Song, S. Cheng, H. Chen, W. Qin, K.-W. Nam, S. Xu, X.-Q. Yang, A. Bongiorno, J. Lee, J. Bai, T. A. Tyson, J. Cho, M. Liu, *Nano Lett.* **2012**, *12*, 3483–3490.

[5] a) X. Lu, M. Yu, G. Wang, T. Zhai, S. Xie, Y. Ling, Y. Tong, Y. Li, *Adv. Mater.* **2013**, *25*, 267–272; b) G. Yu, L. Hu, N. Liu, H. Wang, M. Vosgueritchian, Y. Yang, Y. Cui, Z. Bao, *Nano Lett.* **2011**, *11*, 4438–4442; c) W. Chen, R. B. Rakhi, L. Hu, X. Xie, Y. Cui, H. N. Alshareef, *Nano Lett.* **2011**, *11*, 5165–5172.

[6] a) S. Shi, C. Xu, C. Yang, Y. Chen, J. Liu, F. Kang, *Sci. Rep.* **2013**, *3*, 2598–2605; b) Z. Wang, R. Winslow, D. Madan, P. K. Wright, J. W. Evans, M. Keif, X. Rong, *J. Power Sources* **2014**, *268*, 246–254; c) L. Coustan, A. L. Comte, T. Brousse, F. Favier, *Electrochim. Acta* **2015**, *152*, 520–529.

[7] S. Chen, J. Zhu, X. Wang, *ACS Nano* **2010**, *4*, 6212–6218.

[8] a) M. Irimia-Vladu, E. D. Glowacki, P. A. Troshin, G. Schwabegger, L. Leonat, D. K. Susarova, O. Krystal, M. Ullah, Y. Kanbur, M. A. Bodea, V. F. Razumov, H. Sitter, S. Bauer, N. S. Sariciftci, *Adv. Mater.* **2012**, *24*, 375–380; b) D.-H. Kim, N. Lu, R. Ma, Y.-S. Kim, R.-H. Kim, S. Wang, J. Wu, S. M. Won, H. Tao, A. Islam, K. J. Yu, T.-i. Kim, R. Chowdhury, M. Ying, L. Xu, H.-J. Chung, H. Keum, M. McCormick, P. Liu, Y.-W. Zhang, F. G. Omenetto, Y. Huang, T. Coleman, J. A. Rogers, *Science* **2011**, *333*, 838–843.

[9] G. Zhao, J. Li, L. Jiang, H. Dong, X. Wang, W. Hu, *Chem. Sci.* **2012**, *3*, 433–437.

[10] a) P. Simon, Y. Gogotsi, *Nat. Mater.* **2008**, *7*, 845–854; b) L. Mai, H. Li, Y. Zhao, L. Xu, X. Xu, Y. Luo, Z. Zhang, W. Ke, C. Niu, Q. Zhang, *Sci. Rep.* **2013**, *3*, 1718–1726; c) J. Qian, M. Liu, L. Gan, P. K. Tripathi, D. Zhu, Z. Xu, Z. Hao, L. Chen, D. S. Wright, *Chem. Commun.* **2013**, *49*, 3043–3045.

[11] a) X. Lang, A. Hirata, T. Fujita, M. Chen, *Nat. Nanotechnol.* **2011**, *6*, 232–236; b) Z. Su, C. Yang, B. Xie, Z. Lin, Z. Zhang, J. Liu, B. Li, F. Kang, C. P. Wong, *Energy Environ. Sci.* **2014**, *7*, 2652–2659; c) H. Jiang, T. Sun, C. Li, J. Ma, *J. Mater. Chem.* **2012**, *22*, 2751–2756.

[12] D.-W. Wang, F. Li, M. Liu, G. Q. Lu, H.-M. Cheng, *Angew. Chem. Int. Ed.* **2008**, *47*, 373–376; *Angew. Chem.* **2008**, *120*, 379–382.

[13] a) S. He, C. Hu, H. Hou, W. Chen, *J. Power Sources* **2014**, *246*, 754–761; b) Z. Weng, Y. Su, D.-W. Wang, F. Li, J. Du, H.-M. Cheng, *Adv. Energy Mater.* **2011**, *1*, 917–922; c) W. Wei, X. Cui, W. Chen, D. G. Ivey, *Chem. Soc. Rev.* **2011**, *40*, 1697–1721; d) Y. He, W. Chen, X. Li, Z. Zhang, J. Fu, C. Zhao, E. Xie, *ACS Nano* **2013**, *7*, 174–182; e) L. Yuan, X.-H. Lu, X. Xiao, T. Zhai, J. Dai, F. Zhang, B. Hu, X. Wang, L. Gong, J. Chen, C. Hu, Y. Tong, J. Zhou, Z. L. Wang, *ACS Nano* **2012**, *6*, 656–661.

Received: February 16, 2015
Published online: April 20, 2015

  